Accepted Manuscript

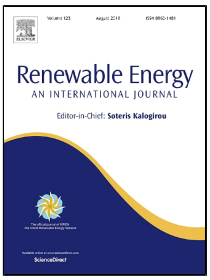

Modelling the hydrodynamic and morphological impacts of a tidal stream development in Ramsey Sound

David Haverson, John Bacon, Helen C.M. Smith, Vengatesan Venugopal, Qing Xiao

PII:	S0960-1481(18)30401-4
DOI:	10.1016/j.renene.2018.03.084
Reference:	RENE 9953
To appear in:	*Renewable Energy*
Received Date:	26 July 2017
Revised Date:	19 March 2018
Accepted Date:	29 March 2018

Please cite this article as: David Haverson, John Bacon, Helen C.M. Smith, Vengatesan Venugopal, Qing Xiao, Modelling the hydrodynamic and morphological impacts of a tidal stream development in Ramsey Sound, *Renewable Energy* (2018), doi: 10.1016/j.renene.2018.03.084

Modelling the hydrodynamic and morphological impacts of a tidal stream development in Ramsey Sound

David Haverson [a,1], John Bacon [a], Helen C.M. Smith [b], Vengatesan Venugopal[c], Qing Xiao[d]

[a] *Centre for Environment, Fisheries and Aquaculture Science, Lowestoft, NR33 0HT*
[b] *College of Engineering, Mathematics and Physical Sciences, University of Exeter, Penryn Campus, TR10 9FE*
[c] *Institute of Energy Systems, University of Edinburgh, Edinburgh, EH9 3DW*
[d] *Department of Naval Architecture, University of Strathclyde, Glasgow, G1 1XQ*

Abstract

A number of sites around the UK are being considered for development of tidal stream energy, one of which is Ramsey Sound off the coast of Pembrokeshire, South Wales. The Sound was used to test the prototype of the Delta Stream by Tidal Energy Ltd. After initial testing, a 10 MW tidal array was proposed at St David's Head. To investigate any possible environmental impacts of the array due to energy extraction, a case study of the Pembrokeshire coast was performed using a high-resolution depth averaged hydrodynamic model, Telemac2D, to investigate changes to hydrodynamics and morphodynamics. Results show that the proposed array of nine tidal energy converters will cause alterations to eddy propagation leading to changes in the velocity field up to 24km from the tidal array. Changes in morphodynamics are predicted through alterations to the bed shear stress. Changes to the mean and maximum bed shear stress, over a 30-day period, are found to be more localised and extend 12km from the array. These changes indicate that the proposed tidal array will lead to localised sediment accumulation and will act as a barrier to sediment transport, with potential consequences for the benthic ecology of the region.

Keywords: Tidal Energy, Tidal Turbines, Ramsey Sound, Hydrodynamic model, Benthic Habitat

1 Introduction

The UK tidal stream energy industry has seen large growth in recent years (RenewableUK, 2015). The number of pre-commercial scale devices currently being tested at test facilities, such as the European Marine Energy Centre (EMEC) in Orkney, reflects this development, however, the ability to commercialise this technology remains a challenge. Even the established UK wind industry still faces significant issues, with numerous Round 3 offshore wind developments halted on grounds of environmental impacts, and the tidal industry is likely to encounter similar challenges. Round 3 sites are the third and latest set of lease sites designated by the UK Government that are consented for development. They reflect the current state of the offshore wind industry, utilising the most state-of-the-art technology and best practices in the UK. Despite numerous proposed array scale projects, some still fall to monetary barriers (reNEWS, 2014), and those that pass these barriers face an increasing challenge to show that their environmental impacts will be minimal. Unlike the wind industry, where physical effects of wind turbines have been catalogued through the deployment of thousands of turbines, the tidal industry lacks such array-scale quantitative data. The MeyGen development in Orkney has been operating the first four turbines, since February 2017 as part of a phased development. It will be the first to provide such datasets.

Many of the impacts are qualitatively known but of great importance is a thorough understanding of the scale of the impacts and their relative significance. Research studies have demonstrated how individual turbines and array scale developments will potentially alter the ecological environment (e.g. Shields et al., 2009; Shields et al., 2011; Miller et al., 2013). In summary, a tidal turbine decreases the near field current flow directly in its wake through energy extraction and the drag caused by the physical structure. The turbine will also affect the far field hydrodynamics, altering the spatial variability of turbulence. The likely consequences of this interaction are alterations to bed characteristics, sediment transport regimes and suspended sediment concentrations.

[1] Corresponding Author:
E-mail address: david.haverson@cefas.co.uk

As bed shear stress is proportional to the square of velocity, the seabed is sensitive to small changes in the current. Environmental monitoring of the Marine Current Turbine (MCT) SeaGen device, in Strangford Loch, concluded that it can "operate with no likely significant impacts on the marine environment" (Keenan et al., 2011). However, it is unlikely that the effects of a single device will be representative at array scale. There is a close relationship between the physical benthic substrate, hydrodynamics and the benthic organisms that dictates where different species are found. Due to high site fidelity, the benthos are easy to examine spatially and temporally meaning they are ideal subjects for studying the impacts of disturbances (Arntz et al, 1999). However, as many benthic species are either sessile (non-mobile) or semi-sessile, they are at greater risk to changes in the physical benthic habitat.

A number of sites around the UK are being considered for development, one of which is the Ramsey Sound, southwest Wales, where flows are accelerated in a channel between Ramsey Island and the mainland. In 2011, Tidal Energy Ltd (TEL) was given consent to test a prototype of their DeltaStream device in Ramsey Sound. The prototype is full scale but consists of only one of the three intended 400 kW rotors mounted on the support structure. The triangular gravity base is 36m wide (Tidal Energy Ltd, 2012). The device was deployed for testing in December 2015 (Tidal Energy Ltd, 2015). Following successful testing, TEL intended to develop a 10 MW demonstration array just north of the Sound at St David's Head. However, since completing this study, TEL went into administration in October 2016. Whilst this particular development is now unlikely to occur, the results of this study are still applicable. The site still has suitable tidal resource and the results give an indication to the scale of impact to a similarly sized array using a different turbine manufacturer. The proposed 10 MW array consisted of nine devices, each with three rotors mounted on the nine individual support structures. Figure 1 shows the boundaries of the lease sites overlaying the bathymetry. The complex bathymetry of Ramsey Sound includes a deep trench (~70m) running north-south, a rocky reef called The Bitches extending west-east from Ramsey Island into the Sound and during a low spring tide a semi-submerged rock pinnacle in the centre of the channel called Horse Rock, approximately 50m in diameter. To the west of Ramsey Island are islets known as the Bishop & Clerks. Within the St David's lease site, depths vary between 32-42m. The tidal range at the site is 5m during springs with a peak spring velocity of 3m/s (Evans et al., 2015). The UK Meterological Office Wave Watch III Hindcast shows waves are predominantly from the south-west with wave heights of 4-5m (Tolman, 2009). The seabed consists of exposed bedrock, gravel and coarse sand (Tidal Energy Ltd, 2012).

Previous work examining tidal energy potential at Ramsey Sound has focused on characterisation of the wider resource through field measurements (Fairley et al., 2013). A detailed assessment of velocities through Ramsey Sound focused on the impact of Horse Rock and the likely environment the single prototype would experience (Evans et al., 2015). It showed that the local bathymetry significantly influences the local velocities causing a velocity reduction in the wake of Horse Rock. This introduces a source of turbulence and areas of vertical tidal flows resulting in a complex vertical velocity profile that may not be ideal for power production from a single tidal turbine in Ramsey Sound. Previously developed numerical models have included Ramsey Sound as part of a wider numerical model of the Irish Sea. In the Lewis et al. (2015) model the resolution is 278m at its finest meaning many of the islands and key bathymetric features are smoothed out as they smaller than the mesh elements. In Walkington & Burrows (2009) the tidal turbines neglect the drag effect of the support structure. A specific model of Ramsey Sound was presented by Fairley et al. (2011). However, the focus of the model was power potential and does not include any tidal turbines. There are presently no studies with sufficient resolution to model the dominant bathymetric features or any studies looking at how the local hydrodynamics and morphodynamics will alter with the presence of tidal turbines at St David's Head.

This paper investigates how a 10 MW tidal array, situated off St David's Head, influences local hydrodynamics using a high-resolution depth averaged hydrodynamic model. The aim is to determine the spatial extent of hydrodynamic change around Ramsey Sound and the potential morphological change.

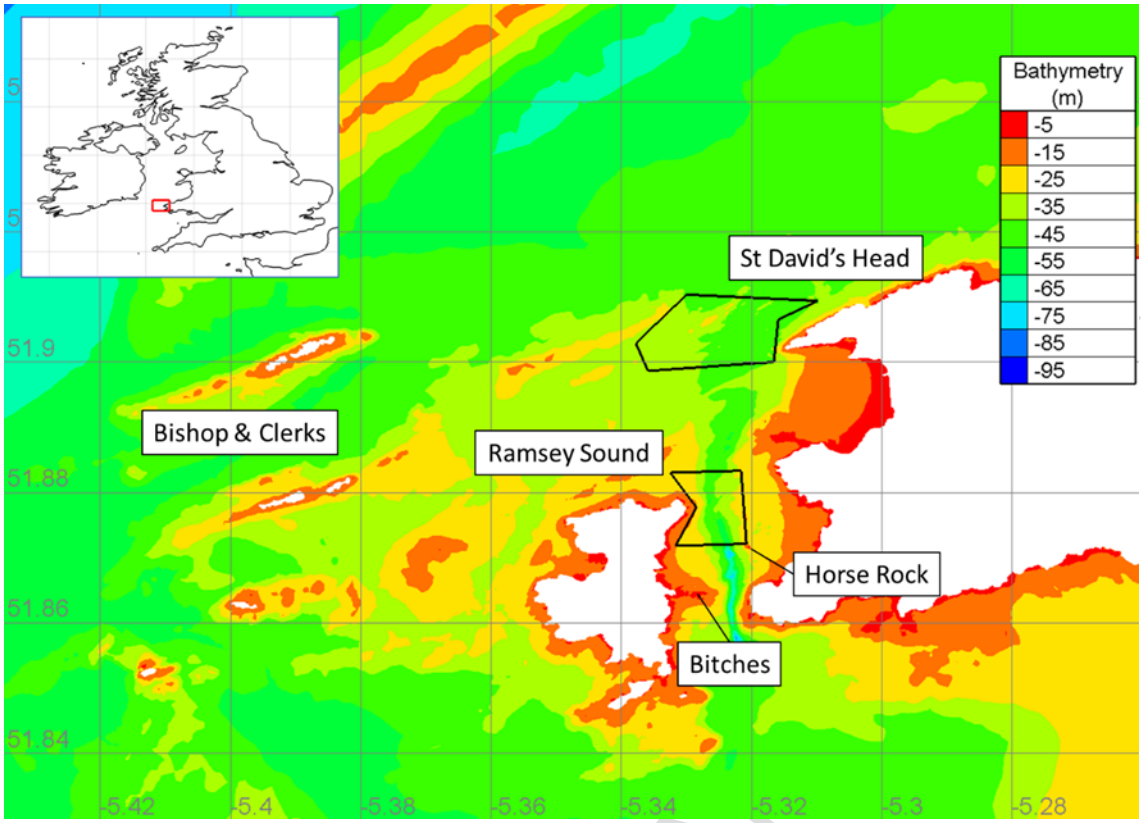

Figure 1: Location of initial test site (bottom) and 10 MW lease site (top), overlaying bathymetry.

2 Methodology

2.1 Numerical model

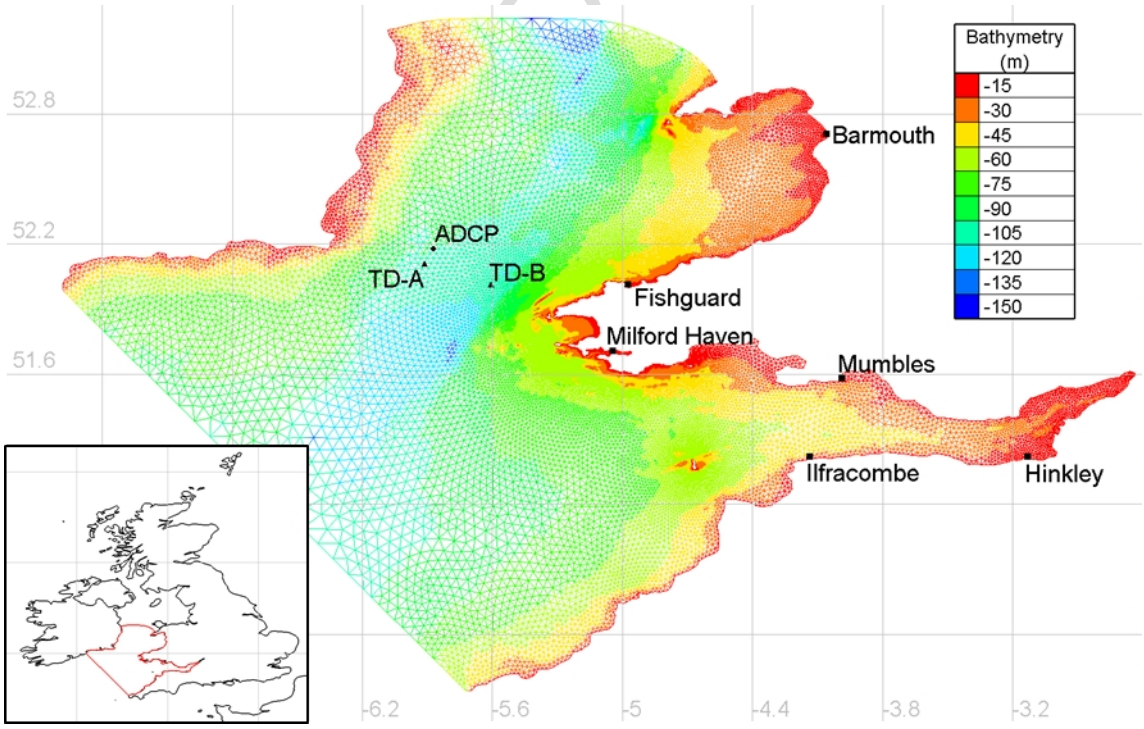

Figure 2: Model computational domain with the location of six tide gauges, two tidal diamonds and one bottom mounted ADCP used for validation.

A high-resolution depth-averaged model of the Pembrokeshire coast was built with an unstructured triangular mesh, using the hydrodynamic software Telemac2D (v7p1). The model domain extends between 50.1°N – 53.2°N and 2.6°W – 7.6°W and is shown in Figure 2. The unstructured mesh was discretized with 138,378 nodes and 271,676 elements. The mesh has a resolution of 10km around the open boundary, reducing to ~2km along the coastline. Along the Pembrokeshire coastline, the resolution increases to ~500m and in areas of interest, such as Ramsey Sound and Stroma Sound, the resolution is refined further to 50m. Around areas of key bathymetric influence within the Sound, such as Horse Rock and the Bitches, the resolution increases further to ~10m.

Bathymetry of the area was sourced from the Department for Environment, Food & Rural Affair's UKSeaMap 2010 (McBreen & JNCC, 2011). The resolution of the bathymetry points from this dataset are 1 arc-second (~30m). However, as bathymetry strongly influences hydrodynamic characteristics through Ramsey Sound, a high resolution 2m and 4m bathymetry, from the UK Hydrographic Office, has also been applied around Ramsey Sound and the Bishop & Clerks. The bathymetry was corrected for mean sea level (MSL) vertical datum using the Vertical Offshore Reference Frame (Iliffe et al., 2013).

The hydrodynamics are forced along the open boundaries using tidal constituents from the OSU TPXO European Shelf 1/30° regional model. The open boundaries are set far from the area of interest to reduce any dampening effect from the prescribed elevations. The Bristol Channel has been included due to its large tidal range and interaction with the Irish Sea because of the geometry of the channel and its quarter wave length resonance to the Atlantic tidal wave (Serhadlioglu, 2014). The model uses a k-ε turbulence model. The depth-averaged parameterisation of k-ε in Telemac was developed by Rastogi and Rodi (1978) with velocity diffusivity set to 1×10^{-6} m^2/s, representing the kinematic viscosity of water. The Nikuradse law for bottom friction was used, with a constant value of roughness length, k_s =0.04, applied to the whole model domain. A bottom friction coefficient k_s=0.01 was initially chosen. However, after repeated runs, a value of ks = 0.04 was found to give the best validation, with the resulting validation shown in Section 3.

2.2 Modelling tidal turbines

Telemac solves a 2D flow using the Saint-Venant equations. The effect of a tidal array is introduced into the model as an extra sink in the momentum equations. This has become the common method for modelling tidal turbines (Ahmadian et al., 2012; Neill et al., 2012; Robins et al., 2014). A tidal turbine causes a change in momentum in two parts: a thrust force produced by the rotor due to energy extraction and a drag force caused by the supporting structure, i.e.-

$$F_{TOTAL} = F_T + F_D = \frac{1}{2}\rho C_T A_r U^2 + \frac{1}{2}\rho C_D A_s U^2, \qquad (1)$$

where U is the upstream velocity, ρ is the density of sea water, C_T is the thrust coefficient, C_D is the drag coefficient, A_r is the swept area of the rotor and A_s is the frontal area of the support structure. The operation and output of the turbine is controlled by the pitch of the rotor blades, resulting in changes in the thrust and power coefficient. The methodology used to represent the operation of the tidal turbines is presented by Plew & Stevens (2013). Below the cut-in speed, the rotor produces no power, meaning that the thrust and power coefficient are set to zero, i.e. $C_T = C_P = 0$. Between the cut-in speed, U_C, and the rated speed, U_D, it is assumed the pitch of the rotor blade is fixed along with the tip speed ratio, resulting in a constant thrust and power coefficient, C_{T0} and C_{P0}. Above the rated speed, the pitch of the rotor blade is increased to reduce the power produced and maintain the rated power, P_D. The power coefficient is parameterised as:

$$C_P = \frac{2P_D}{\rho A_r U^3}, \quad U > U_D, \qquad (2)$$

For simplicity, Plew and Stevens (2013) assume a fixed relationship between the thrust and power coefficient, resulting in the thrust coefficient above rated speed being parameterised as:

153 $$C_T = \frac{C_{T0}\ 2P_D}{C_{P0}\rho A_r U^3}, \quad U > U_D, \qquad (3)$$

154

155 The values and constants, used for this study, are based on the published figures of the TEL
156 DeltaStream device (Tidal Energy Ltd, 2012). Each device consists of three 400kW rotors with a
157 diameter of 15m. Each rotor reaches its rated power output at a current velocity of 2.25m/s. Based upon
158 these parameters, the values for the constant power and thrust coefficients are $C_{P0} = 0.29$ and $C_{T0} = 0.8$.
159 The simulated 10 MW array contains 9 devices with 27 rotors. Whilst the actual array layout is yet to
160 be finalised, the preferred option was to arrange the turbines in three rows of three situated to the east
161 of the lease site due to the shallower depths and associated increased current speeds (Tidal Energy Ltd,
162 2012). The hub height is 14m. It has been assumed that the rotor has a cut-in speed of 0.8m/s. For
163 simplicity, the vertical support structure has been modelled as a cylindrical monopile with a diameter
164 of 2m and a drag coefficient $C_D = 0.9$. In the area where the turbines are modelled, a regular mesh using
165 triangular elements is used ensuring any variation is due to the hydrodynamics and not the mesh
166 (Haverson et al., 2017). The resolution of these regular meshes is 20m. Each device is represented
167 individually, with the force of each device spread over eight elements.

168 ## 3 Validation

169 ### *3.1* *Free surface elevations*

170 Validation data have been obtained from the British Oceanographic Data Centre (BODC) for
171 surface elevation at six tide gauges, whose locations are shown in Figure 2. The model was run for 30
172 days from 17/05/2012 00:00 to 16/06/2012 00:00. Comparisons of the modelled free surface elevation
173 and observed tidal elevations, at Barmouth, Fishguard, Milford Haven, Mumbles, Ilfracombe and
174 Hinkley, are shown in Figure 3.

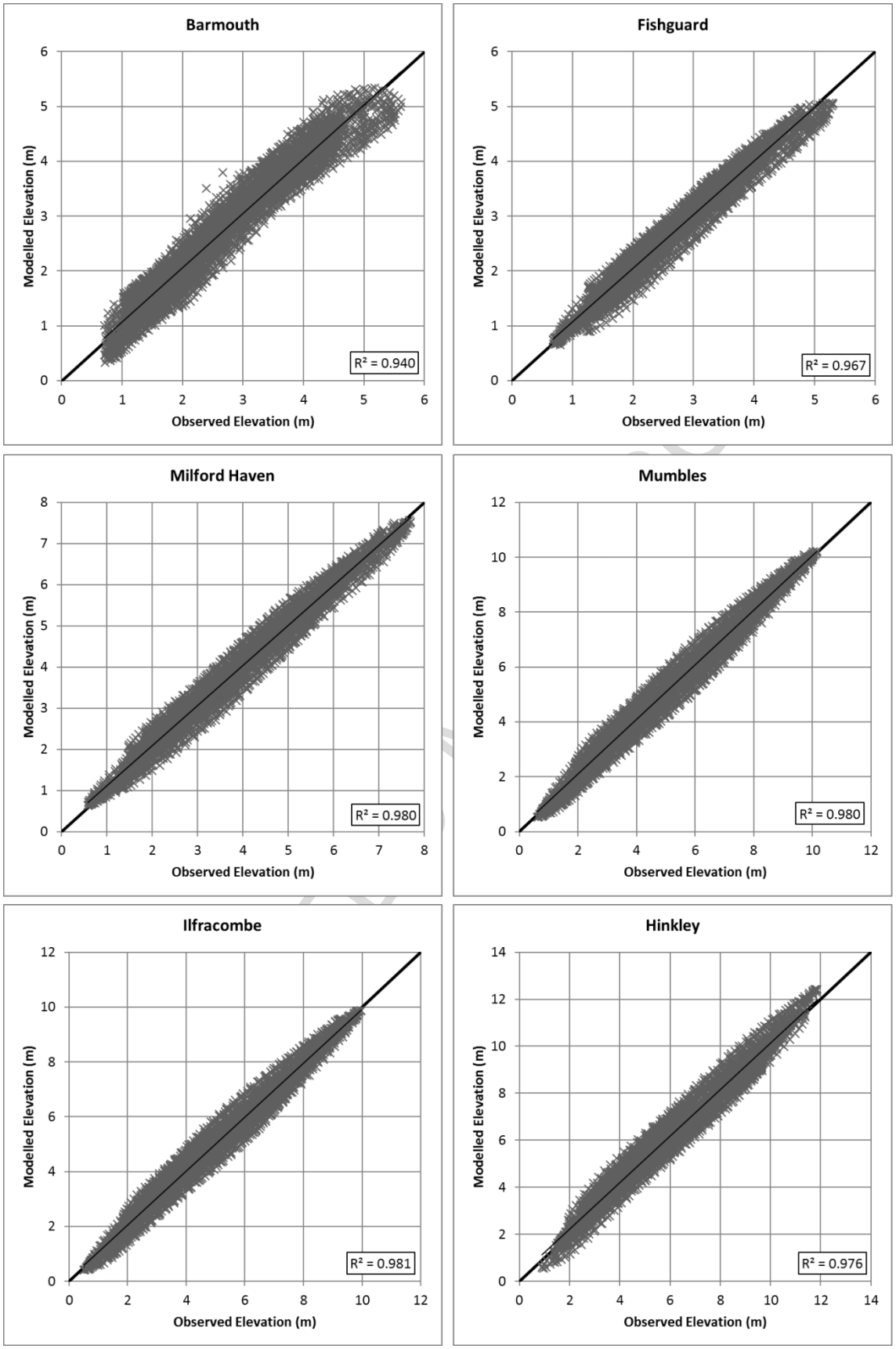

Figure 3: Comparison of modelled free surface elevation and observations from BODC tide gauges. The black line represents a y=x relationship.

The scatter plots show good agreement for Fishguard, Milford Haven, Mumbles, Ilfracombe and Hinkley. A broader scattering is seen in the Barmouth comparison due to a slight phase misalignment. This could be due to the Afon Mawddach estuary being clipped from the model to improve computation speed. To validate the free surface elevations, three statistical tests have been applied: the coefficient of determination, the root mean squared error (RMSE) and the scatter index. The scatter index is the RMSE normalised by the mean of the observations. It is widely used in the validation of wave models (Cox & Swail, 2001; Niclasen & Simonsen, 2007; van Nieuwkoop et al., 2013), meaning there is a wide source of literature for comparable values. However, there is no comparison for validating tidal elevations. For this study, a scatter index of less than 10% will be considered a good validation. Table 1 summarises the validation statistics of the six tide gauges.

Table 1: Validation statistics of the six tide gauges.

Tide Gauge	R^2	RMSE (m)	Scatter Index (%)
Barmouth	0.940	0.296	10.99
Fishguard	0.967	0.196	7.18
Milford Haven	0.980	0.250	6.38
Mumbles	0.980	0.353	6.81
Ilfracombe	0.981	0.329	6.59
Hinkley	0.976	0.478	7.70

It can be seen from the validation statistics that model validates very well. The R^2 show a very strong correlation between the modelled and observed free surface, with an average of 0.971. It can be seen from the scatter index that all the tide gauges show good agreement, except for Barmouth, which is just outside the acceptable range.

3.2 Velocities

The area of greatest interest within the model domain is St David's Head. The closest dataset that could be obtained for validation was a line transect through Ramsey Sound. Line transects, using a side mounted ADCP, were conducted to determine velocities within Ramsey Sound on behalf of the Low Carbon Research Institute Marine Consortium. Details of the survey methodology and results are published by Evans et al. (2015). To compare the transect with the model results the ADCP record has been depth averaged. Figure 4 shows a comparison between the model and the transect.

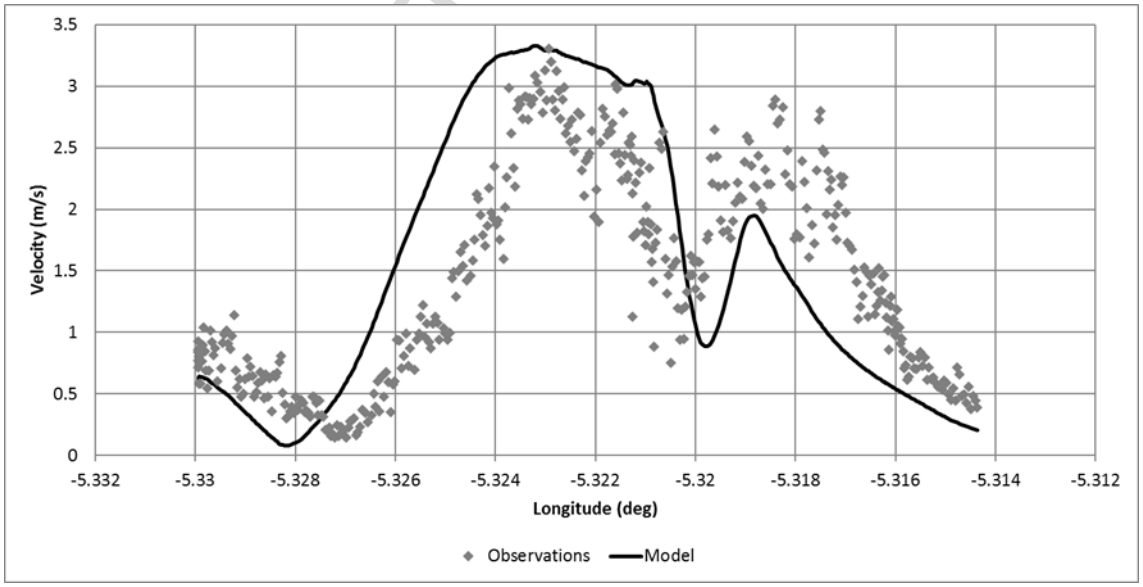

Figure 4: Line transect comparison of modelled and observed depth averaged tidal currents through Ramsey Sound.

The model does reproduce the peak velocity magnitude, of 3.3 m/s, through the centre of the Sound. Likewise, the velocity reduction in the wake of Horse Rock is visible, at the longitude -5.32°. There are some discrepancies between the observed velocity profile and the model. The high velocities east of Horse Rock are under-predicted. It is expected that the model will not entirely match the ADCP transect. The 3D hydrodynamics through Ramsey Sound are strongly influenced by the local bathymetry meaning there are inherent limitations to all depth averaged models of this sort being able to accurately reproduce real 3D conditions (Evans et al., 2015). What is important for this study is the model reproduces the peak magnitude, which in this instance is correctly modelled.

Along with six tide gauges, BODC provided a 30-day bottom mounted ADCP time series recorded between 17/05/2000 – 17/06/2000. The ADCP was located at 52°10.6N 5°52.3W and is shown in Figure 2. The observed velocities have been depth averaged to compare against model results. Whilst the date of the ADCP record is the same month as the tide gauges and the model run, the ADCP was deployed two years earlier meaning a direct comparison of the time series cannot be made. However, the ADCP record length is sufficient to cover a full spring-neap cycle so a comparison of both the peak magnitude and direction is possible. Figure 5 shows the comparison of the observed and modelled depth averaged velocities at the location of the ACDP. It can be seen that the two time series show good agreement. The peak velocities for the ADCP is 1.43 m/s and 1.53 m/s for the flood and ebb respectively. The peak velocities from the model are 1.43 m/s and 1.58 m/s for the flood and ebb respectively.

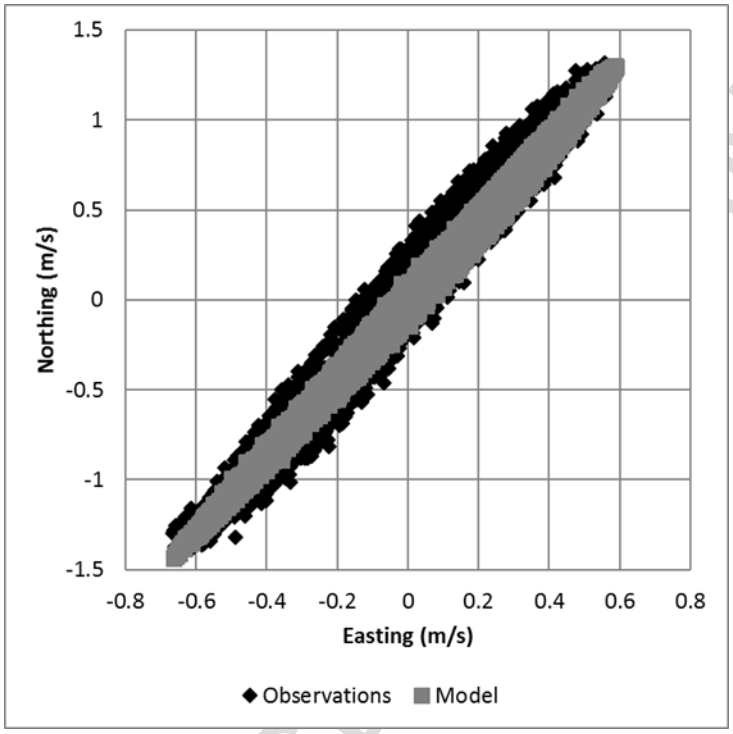

Figure 5: Comparison of observed and modelled depth averaged velocities situated at 52°10.6N 5°52.3W.

Velocities were further validated using tidal diamonds from United Kingdom Hydrographic Office (UKHO) Admiralty Chart 1121. The location of the two tidal diamonds are shown in Figure 2. Figure 6 shows the comparison between the modelled and observed tidal velocities and direction six hours either side of high water during a spring and neap cycle. High water is taken with respect to Milford Haven. The direction is that of the spring velocities. Results show good agreement between the model and the tidal diamonds.

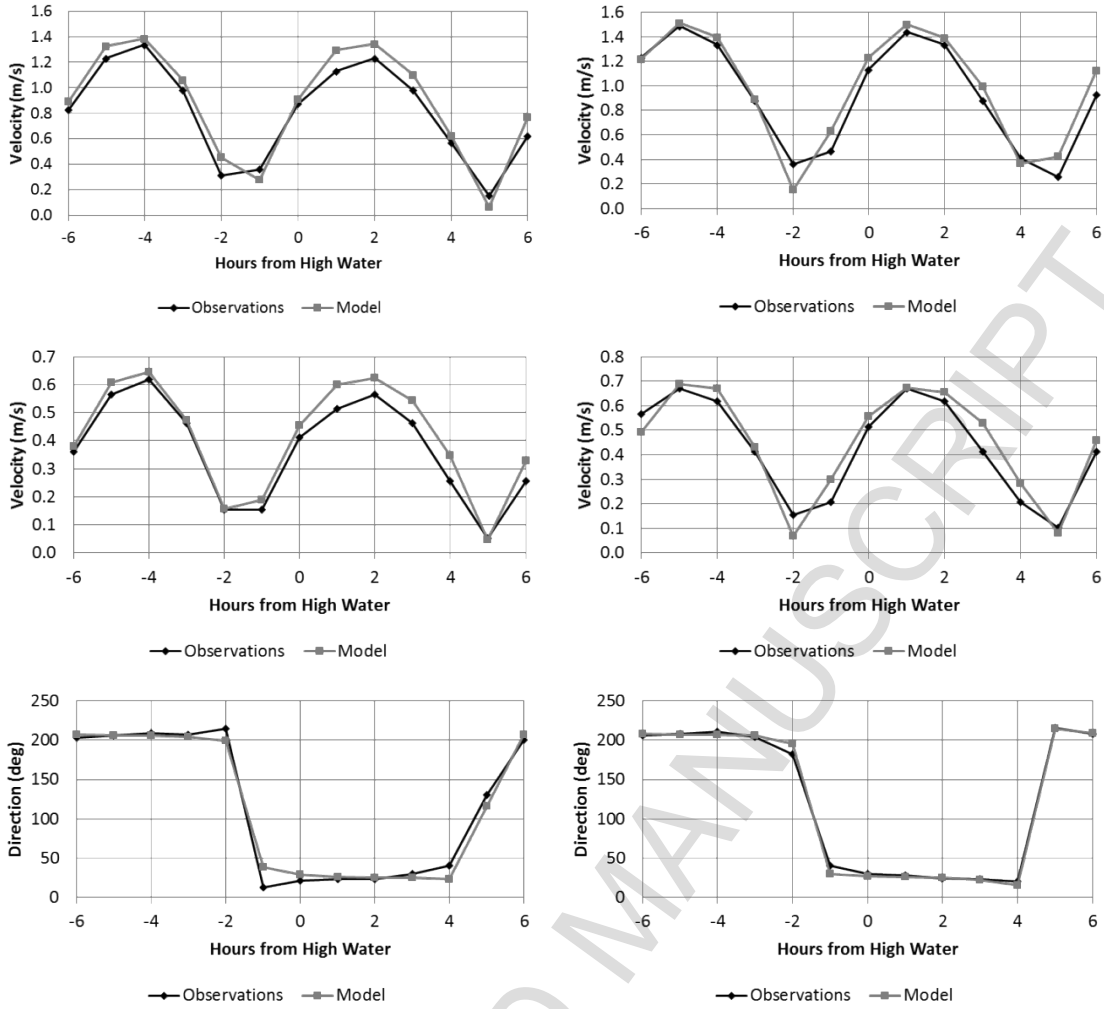

Figure 6: Comparison between modelled and observed velocities at spring (top), neap (middle) and direction of spring velocities (bottom) of two tidal diamonds from UKHO Admiralty Chart 1121 (a-left, b-right). High water is with respect to Milford Haven.

3.3 *Harmonic analysis*

The model was run for 30 days to provide a time series of sufficient length to permit a harmonic analysis which includes the dominant components. The dominant components are the M2 and S2 constituents. Table 2 and Table 3 show the comparison between harmonic constituents from the UKHO and the model for the M2 and S2 constituents at UK ports.

Table 2: Comparison between observed and modelled M2 constituent.

Port	M2					
	Observed Amplitude (m)	Model Amplitude (m)	Percentage Difference	Observed Phase (deg)	Model Phase (deg)	Percentage Difference
Fishguard	1.35	1.34	-0.7%	207	206.9	-0.1%
Porthgain	1.33	1.39	4.5%	197	195.9	-0.6%
Ramsey Sound	1.46	1.47	0.7%	185	185.2	0.1%
Solva	1.89	1.89	0.0%	178	178.4	0.2%
Martin's Haven	1.84	1.86	1.1%	180	177.7	-1.3%
Milford Haven	2.22	2.22	-0.9%	173	171.9	-0.6%
Mumbles	3.18	3.19	0.3%	171	171.2	0.1%

240 **Table 3: Comparison between observed and modelled S2 constituent.**

Port	S2					
	Observed Amplitude (m)	Model Amplitude (m)	Percentage Difference	Observed Phase (deg)	Model Phase (deg)	Percentage Difference
Fishguard	0.53	0.51	-3.8	248	248.1	0.0
Porthgain	0.52	0.52	0.0	239	238.6	-0.2
Ramsey Sound	0.51	0.53	3.9	238	229.4	-3.6
Solva	0.75	0.68	-9.3	225	222.8	-1.0
Martin's Haven	0.68	0.67	-1.5	224	222.3	-0.8
Milford Haven	0.81	0.78	-3.7	217	216.8	-0.1
Mumbles	1.12	1.12	0.0	221	219.1	-0.9

241

242 Results of the harmonic analysis show that the M2 and S2 constituents validate for both amplitude and
243 phase. The only discrepancy is with the S2 amplitude at Solva which is under-predicted. This could be
244 due to the Solva inlet being clipped from the model domain to reduce computation run time. The
245 validation results over the remaining model domain show good agreement.

246 ## 4 Results and discussion

247 ### *4.1 Array performance*

248 The performance of the array has been assessed through the predicted energy production. Results of
249 the simulation show that over the spring-neap cycle the total output of the array is 2.15 GWh. This
250 equates to 25.80 GWh per annum. The energy production is not uniform across the array. Figure 7
251 shows the array layout and the numbering convention of the devices. Devices 1, 2 and 3 represent row
252 1; devices 4, 5 and 6 represent row 2 and devices 7, 8 and 9 represent row 3. Devices 1, 4 and 7 represent
253 column 1; devices 2, 5 and 7 represent column 2 and devices 3, 6 and 9 represent column 3.

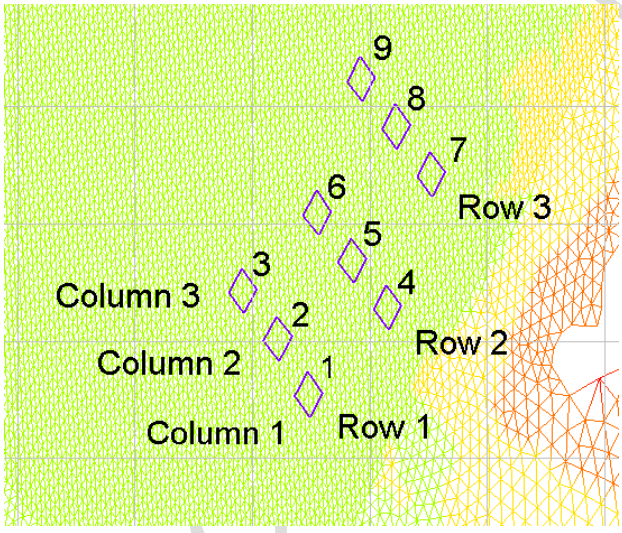

254

255 **Figure 7: Device number convention.**

256 Figure 8 shows the total energy production of each device with respect to their position within the
257 array. Figure 9 shows the power produced by Device 1 and 9 representing the smallest and largest
258 producing devices, respectively.

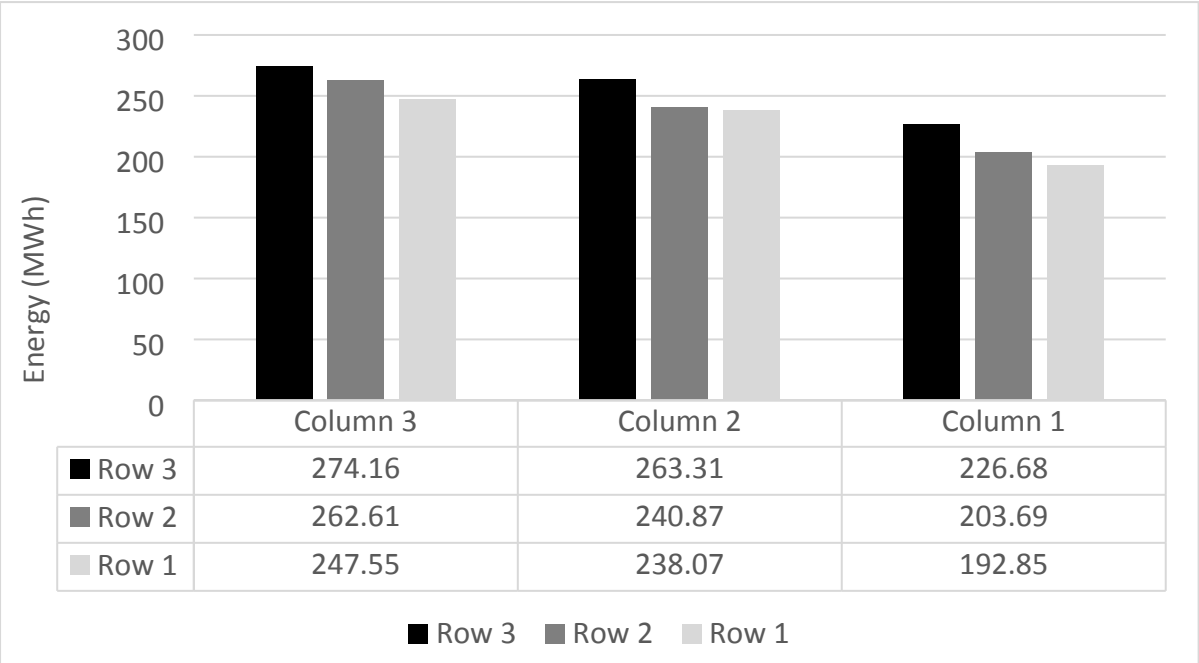

Figure 8: Total energy (MWh) produced over a spring-neap cycle.

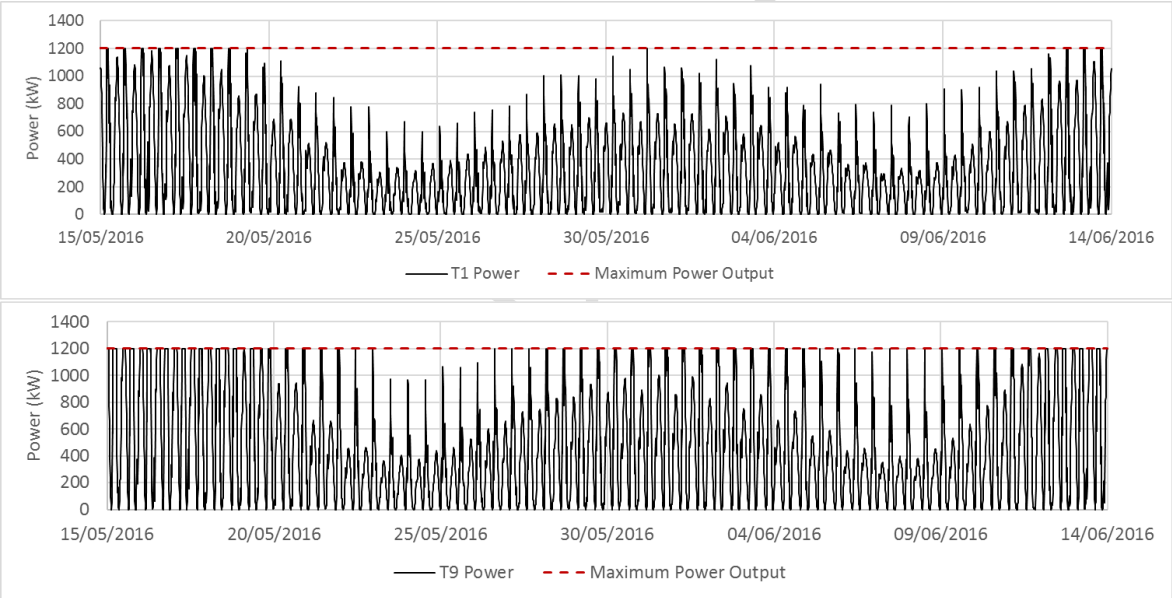

Figure 9: Power production from the Device 1 (top) and Device 9 (bottom) representing the smallest and largest producing devices, respectively, over the 30-day model run. Red dashed line represents the maximum instantaneous power production per device (1200 kW).

Device 9 reaches rated power regularly over the whole spring and neap cycles, whereas, Device 1 rarely reaches rated power. This is because the flow speed at this location rarely exceeds 2m/s, less than the rated speed. The strong tidal asymmetry between the flood and ebb cycle is clearly shown in the power output in Figure 9, with the ebb cycle producing a third less power than on the flood. The strong tidal asymmetry of the site is caused by the combination of the M2 tidal constituent and its higher harmonic the M4 constituent (Pingree & Griffiths, 1979).

4.2 Influence of tidal array

To assess the influence of the 10 MW tidal array, a harmonic analysis was conducted on the base case (without any turbines placed within the model) and the turbine case (with the nine turbines

included). By comparing the two cases, it was possible to examine the spatial extent and magnitude of change to the principal M2 and S2 tidal constituents caused by the presence of the array. Figure 10 shows the changes to the M2 and S2 tidal velocity constituents, with the dashed lines representing contours of a 2% and 5% amplitude reduction.

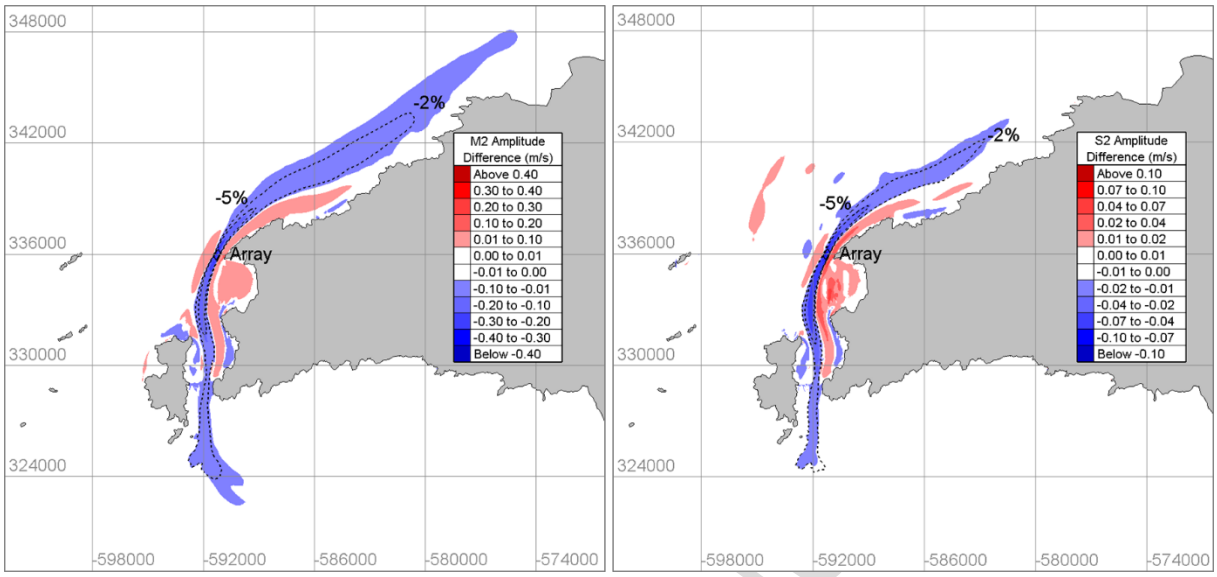

Figure 10: Changes to the M2 (left) and the S2 (right) tidal velocity constituents. The dashed lines represent contours of a 2% and 5% amplitude reduction.

Using a 5% reduction contour, the reduction in the M2 amplitude in the wake of the array extends 3km north and 4.5km south. Using a 2% reduction contour, the influence of the array extends further to 13km north and 12km south. For the S2 amplitude, the wake extends 3.5km north and 5km south using a 5% reduction contour and extends 10.5km north and 12km south at 2%. The largest reduction to the amplitude of the M2 tidal velocity constituent was at Device 9 with 0.41 m/s. This is equivalent to a 19.8% reduction. However, the largest percentage change occurred at Device 1 with a 0.36 m/s reduction, equivalent to 20.3%. For the S2 constituent, the largest percentage reduction also occurred at Device 1 with 18.9%. Black & Veatch (2005) used the term, 'Significant Impact Factor' (SIF), to quantify a percentage of the total (kinetic energy) resource at a site that could be extracted without significant economic or environmental effects. They suggest a value of 20%. Using the flux method outlined in Black & Veatch (2005), the potential resource of St David's Head is 52.7 MW. Applying a SIF of 20% gives an available resource of 10.5 MW. The results gained in this study therefore, suggest that the size of the development is acceptable, with respect to the SIF, but the size of the development should not grow beyond 10 MW without risking a greater impact.

4.3 Hydrodynamic far field effects

Ramsey Sound experiences a very turbulent environment due to complex bathymetry of the area and there are many sources of disturbance to the flow. The largest source of turbulence is Ramsey Island itself, where the flow of water through the Sound re-joins the main flow around the west of the island. Robinson (1981) describes that when two separate streams of flow with different stagnation pressure or total head meet at a sharp headland it can lead to a discontinuity in velocity. This discontinuity is a vortex line that gradually diffuses into the surrounding water. It can be seen in the model that large eddy structures form off Ramsey Island on the flood cycle, propagating northwards along the coastline. When the influence of the tidal array is introduced, the wake of the array alters the production and propagation of the eddies, such that resulting change during the ebb flow influences the next cycle of eddy formation on the flood. This new disturbance then cyclically continues to alter the surrounding flow changing how other eddies propagate from other sources, such as the Bishop & Clerks. These disturbances can travel significant distances and can be used to characterise the far field effects, as seen in Figure 11. Since

there are no sources of eddy generation north of the array (i.e. islands or rock features) the disturbance to eddy generation and propagation is more prominent to the south.

Figure 11 shows the zone of influence as calculated by the normalised range of difference. The range of difference is calculated by subtracting the magnitude of velocity at each node of the mesh of the turbine run from the magnitude of the velocity in the base case. This is done for each time step, producing a temporally and spatially varying difference between the two models. The range of difference is the difference between the maximum increase and decrease at each node over the whole model run. The range is then normalised to the maximum change to give a percentage figure. The range of difference does not represent the instantaneous velocity reduction due to the direct wake of the turbine array at any one time. Instead, it gives an indication of the total temporal and spatial extent of change. A value of 5% has been chosen to delineate the outer extent of the zone of influence. It can be seen that the zone of influence of the tidal array extends 24km south west and 19km north east of the array.

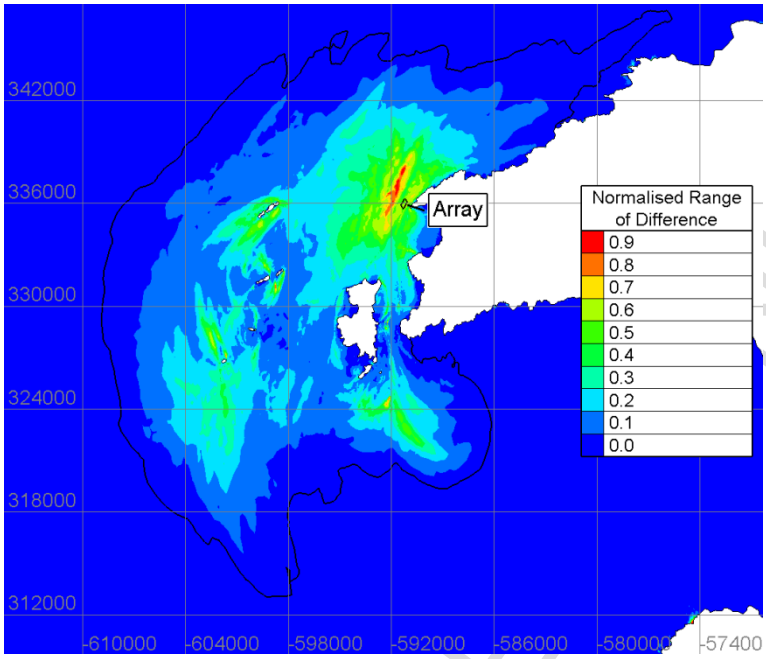

Figure 11: The zone of influence (black line), as characterised by the far field effects, of the 10 MW array at St David's Head.

4.4 Morphological effects

The principal effects of a tidal turbine on the morphodynamics are alterations to bed characteristics, sediment transport regimes and suspended sediment concentrations. Where strong flows occur, sediments are re-suspended readily, deposition is minimal and the bed is commonly eroded down to hard strata with no laminae of overlying sediment. British Geological Survey (BGS) maps show that the wider area around Ramsey Sound is predominantly a mixture of sand and gravel, with a larger proportion of gravel. St Brides Bay consists of a mixture of fine sand and mud due to low tidal velocities that circulate just within the bay. Figure 12 shows the seabed sediments within the model domain based upon 1:250,000 digital sea-bed sediments map (DigSBS250).

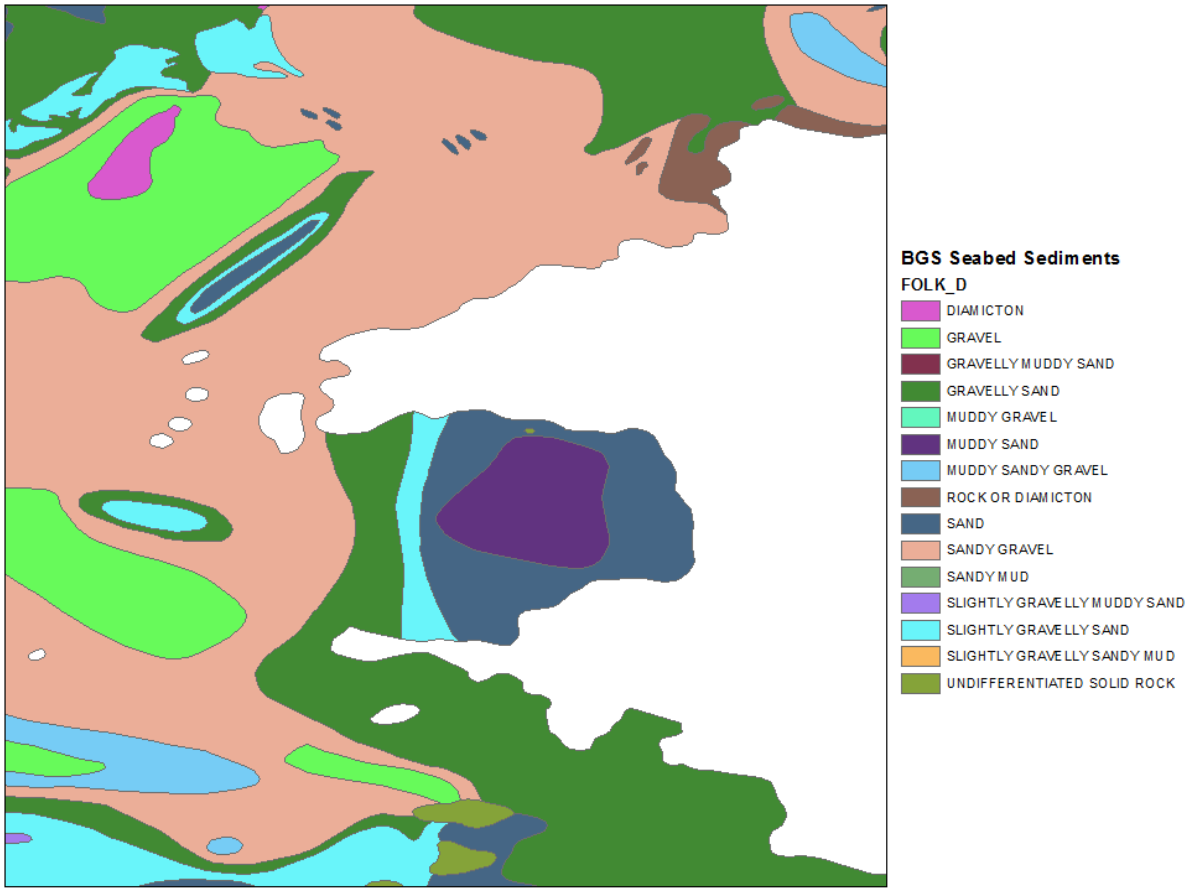

Figure 12: BGS Seabed Sediments using the Folk Classification. Reproduced with the permission of the British Geological Survey ©NERC. All rights Reserved.

The types of sediments found around Ramsey Sound suggests the area directly around a tidal array would not change greatly because of the absence of smaller sediments. Therefore, the far field effects shown in the model are likely to have a greater impact on sediment dynamics in the more benign hydrodynamic conditions away from the tidal array. It is important to note that this is a purely tidal hydrodynamic model with no atmospheric forcing or wave driven currents. The position and dispersion of eddies in this area would naturally vary if these additional interactions are included. A clearer indicator of potential impact is the change to bed shear stress as this is the parameter that drives the alterations to sediment dynamics. Bed shear stress is calculated as:

$$\tau = \rho C_d ||U|| U. \qquad (4)$$

where ρ is the density of seawater, C_d is the bottom drag coefficient and U is the velocity. For this study, a constant drag coefficient of 0.0025 was chosen representing a sand/gravel environment (Soulsby, 1997). This also matches the value used by Martin-Short et al (2015).

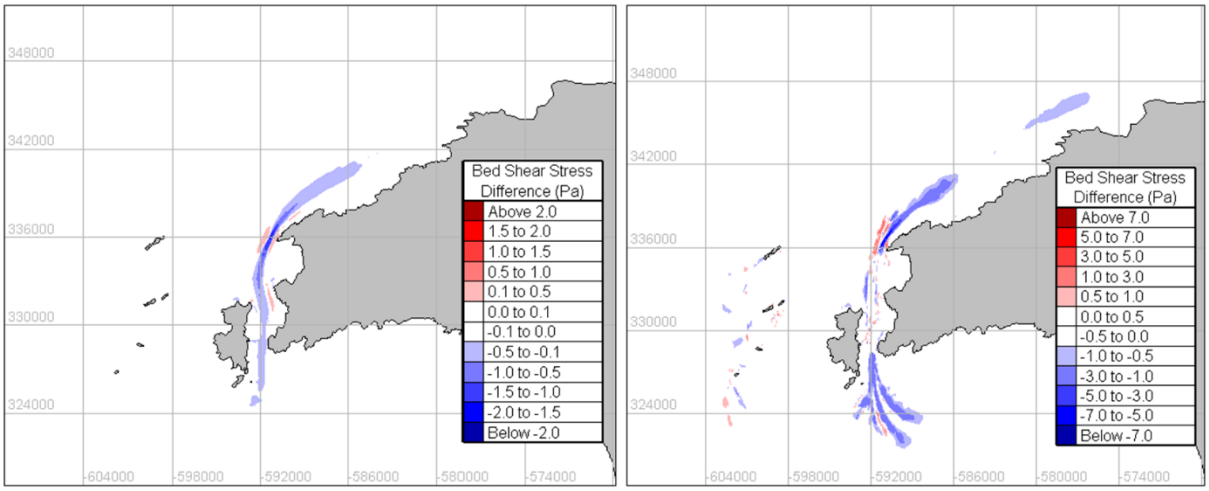

Figure 13: Change in mean (left) and maximum (right) bed shear stress.

Figure 13 shows the change to the mean and maximum bed shear stress, respectively, over the 30-day simulation. The results show the spatial extent of the change due to the tidal array is more localised than Figure 11 suggests. The presence of the tidal array causes a local reduction in bed shear stress, with effects extending 16km from the site. Over the 30-day model run, the largest mean reduction is 2.3 Pa. The maximum reduction is 7.5 Pa. The resulting change in bed shear stress suggests that an accumulation of sediment may occur within the vicinity of the array where bed shear stress has reduced. Additional scour, between the array and the mainland where the flow is accelerated by constriction due to the impedance of the array, may also occur. Caution should be applied as the alterations to bed shear only show changes to skin friction. More detailed sediment modelling is required to determine the impact on bed feature evolutions and sediment transport.

A full sediment model, with bed evolution and suspended sediments, is difficult to achieve without appropriate sediment flux values at the boundary and sediment layers on the bed. However, Martin-Short et al. (2015) show that bed shear stress is a major controller of sediment movement and an understanding of its distribution over the bed makes an assessment of the sediment transport regime and estimates of the finest grain sizes that will settle to be made. The threshold of motion for a particular grain size (d) can be determined through the threshold shield parameter (θ_c):

$$\theta_c = \frac{\tau_{cr}}{g(\rho_s - \rho_f)d} \qquad (5)$$

where τ_{cr} is threshold shear stress, ρ_s is density of sediment and ρ_f is density of the fluid containing the sediment, in this case sea water. As there are insufficient data for the exact grain size distribution of the model domain, it is difficult to accurately calculate values of θ_c. Instead, values for τ_{cr} for a range of grain sizes have been taken from Martin-Short et al. (2015) and are shown in Table 4. These values were originally referenced by Berenbrock & Tranmer (2008).

Table 4: Mean threshold shear stress (τ_{cr}) conditions for the entrainment of various grain sizes (d) (from Berenbrock & Tranmer, 2008).

Sediment Class	Diameter (mm)	Critical Shear Stress (Pa)	Critical velocity (m/s)
Coarse Gravel	16 - 32	12.2 - 26.0	2.16 - 3.19
Medium Gravel	8.0 - 16	5.7 - 12.2	1.49 - 2.16
Fine Gravel	2.0 - 8.0	1.26 - 5.70	0.70 - 1.49
Coarse Sand	0.5 - 2.0	0.27 - 1.26	0.325 - 0.7
Medium Sand	0.25 - 0.5	0.194 - 0.27	0.275 - 0.375

Figure 14 shows the predicted sediment distribution during the flood and ebb cycle of a peak spring tide. The colouration of each sediment class has been scaled to the values of τ_{cr} in Table 4. The maps

show broad agreement with the sediment mix detailed in the British Geological Survey (BGS) DigSBS250 map, shown in Figure 12.

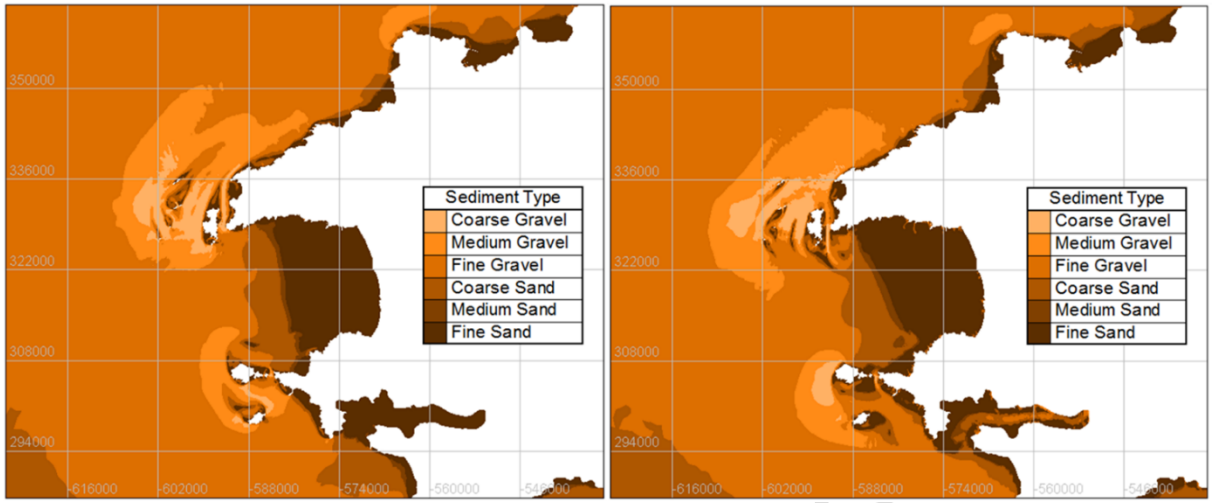

Figure 14: Predicted sediment maps during peak flood (left) and peak ebb (right).

There is a significant difference between the predicted sediment maps (Figure 14) during the flood and ebb suggesting any sediment accumulated over one half of the tidal cycle is likely to be transported over the next half. Figure 15 and Figure 16 show the changes to the sediment maps during a peak flood and ebb with and without the tidal array. Due to the size of the tidal array, the changes to sediment transport are subtle. During the flood, there is a greater accumulation of medium gravel within the array and 1 km downstream in its wake. During the ebb, there is an increased accumulation of fine gravel 3 km downstream of the array at the northern entrance of Ramsey Sound as well as coarse sand north of Ramsey Island. As flow speeds through St David's Head and the Bishop's & Clerks exceed 2m/s, as well as speeds exceeding 3m/s in Ramsey Sound, any sediment smaller than coarse gravel is unlikely to stay within this region for long. Any sediments fed into the area from the north or south are likely to be transported through the region within a few tidal cycles. Therefore, the largest impact the tidal array is likely to have is as a barrier to the net transport of sediment. The width of fine gravel accumulation adjacent to the coastline at St David's Head is larger during both the flood and ebb cycle. The discussion of the results is qualitative in nature as the maps do not allow for quantifiable changes to sediment transport to be assessed, hence, caution should be applied when interpreting the impacts from these sediment maps.

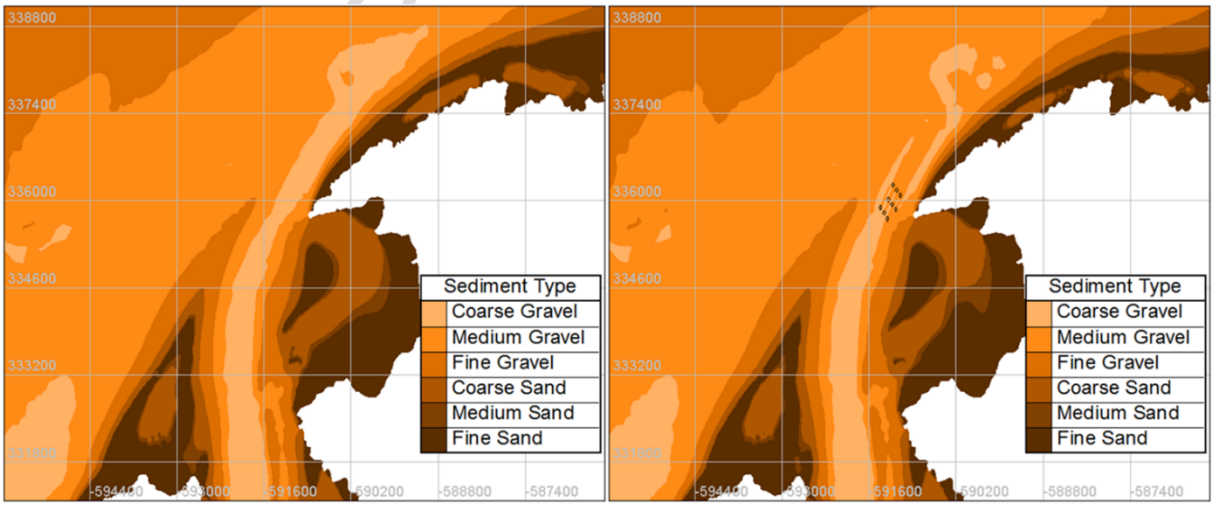

Figure 15: Predicted sediment maps during peak flood with no turbines (left) and 9 devices (right).

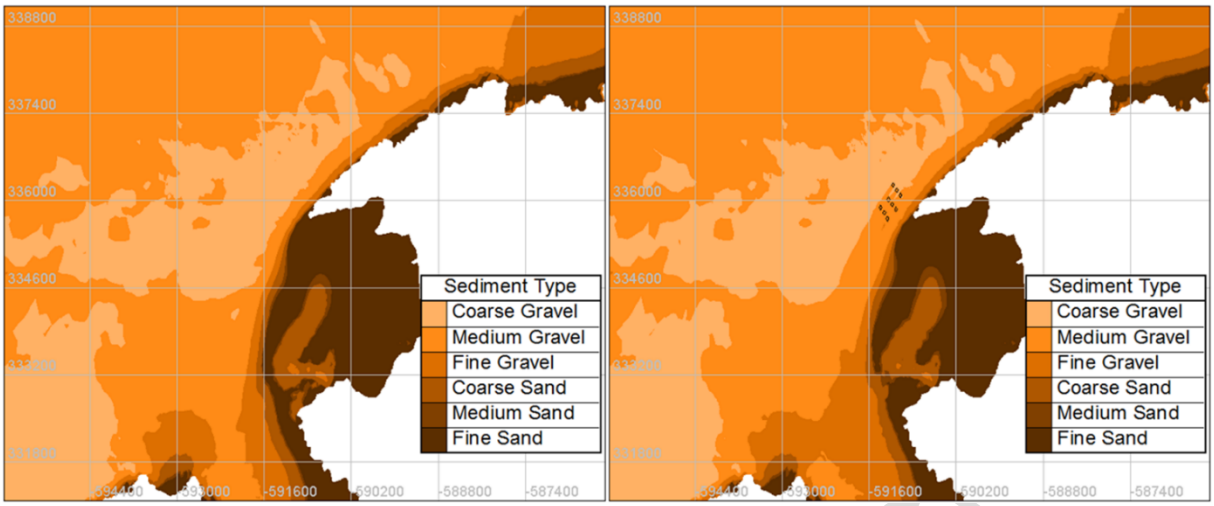

Figure 16: Predicted sediment maps during peak ebb with no turbines (left) and 9 devices (right).

4.5 Discussion

The changes in sediment transport as noted above are likely to impact the benthic environment in a number of ways. The presence of the tidal array results in a potential change in the sediment class distribution that could lead to a change in the physical benthic habitat such that it is no longer favourable to the species presently occupying a particular area. Similarly, an increase in sediment accumulation could lead to the burial of certain benthic species. This has been demonstrated in several studies (e.g. Rogers, 1990; Short & Wyllie-Echeverria, 1996). Although burial from increased sedimentation can lead to mortality, laboratory experiments show that some species can adapt to sediment burial (Hinchley et al., 2006). The model results show the impact is likely to be small and may be potentially positive. The largest reduction in bed shear stress was limited to within the vicinity of the devices, as is seen in similar studies in Pentland Firth and Alderney (Martin-Short et al., 2015; Thiebot et al., 2015). This area is predicted to contain coarse gravel meaning a 7.5 Pa reduction in bed shear stress will result in an accumulation of medium and fine gravel. However, the results should be considered with respect to the fact the model is a depth-averaged model. When using 2D energy extraction, the velocity is reduced over the entire water column. In reality, the vertical profile will be distorted much like the bypass flow around a turbine. Brown et al (2017) showed that the velocity above and below the turbine will be faster than through the rotor plane by as much as 10%, highlighting that the flow beneath the rotor is of importance. This is because the flow is constrained between the turbine and the seabed, which could have implications for sediment transport, that depends on the type of sediments, whether the site is dominated by suspended or bed load sediments. Therefore, the reduction in bed shear stress below the turbines may be smaller than predicted by the depth-averaged model and caution must be taken when applying 2D model results to real sites. As a result, the change in sediment class may not be functionally different.

It is the more hydrodynamic benign areas within the zone of influence of the array that may have a more noticeable effect due to the subtle changes. Small-scale disturbances can create patchiness in resources leading to a greater diversity within a benthic community (Thrush & Dayton, 2002). This in turn is important in creating a fully functioning ecosystem. Many species fill a niche within a system, obtaining resources in different ways. Whilst different species adapt to take on different functions, the relative importance of different species will vary within the system (Covich et al, 1999). The loss of an individual species due to a disturbance may not impact the system providing its function is fulfilled by another species. Depending on the scale of the disturbance, neighbouring species may quickly repopulate the area. A small-scale study of the benthic species assemblage response to the presence of OpenHydro's device deployed at the EMEC showed an increase in the species biodiversity and compositional differences within the device site (Broadhurst and Orme, 2014). It is important to note that investigations like this are site specific and general conclusions should not be drawn. The results presented here contrast with the estimated impact in the Pentland Firth as demonstrated by Martin-Short

et al (2015), where the peak reduction in bed shear stress was 25 Pa and could potentially alter the migration of sandbanks in the area investigated. However, the site investigated had significantly more devices in faster flows (200 MW; 4.5 m/s) meaning the impact was greater.

Due to the high flow speeds and the very turbulent nature of the flow field, Pembrokeshire is an area of medium-high suspended sediment transport (>1 m^2s^{-1}) (Robins et al., 2014). Filter feeders rely on nutrients transported in the suspended sediments. Ahmadian et al (2012) showed that suspended sediment concentrations were altered up to 15km from a tidal stream array modelled in the Bristol Channel. However, the levels of suspended sediments found in the Bristol Channel are much lower than around Pembrokeshire. Anglesey, North Wales, has a similar suspended sediment regime to Ramsey Sound where Robins et al (2014) showed that 50 MW of tidal stream turbines could be installed without changing suspended sediments above natural variation. Additionally, Heath et al. (2016) showed that current speeds would need to change by 50% to cause a detectable change in turbidity. Although suspended sediment levels were not modelled, the small scale of the proposed tidal development at Ramsey Sound means that the reduction in the global suspended sediment rates is likely to be small meaning a minimal impact on filter feeders. Further work is required to determine the ecological response to the change in morphodynamics in Ramsey Sound.

The discussion of the results is qualitative in nature as the predicted sediment maps do not allow for quantifiable changes to sediment transport to be assessed, hence, caution should be taken when interpreting the impacts from these sediment maps. However, they do provide useful insight into the potential changes of sediment pathways and the likely areas of change. This was a similar view of Gallego et al. (2017) who discuss that at the heart of all modelling lies the most appropriate and best quality data. Gallego et al (2017) developed a coupled 3D hydrodynamic and morphodynamics model of the Pentland Firth to investigate tidal energy resource and environmental impact. The results showed similar behaviour in that the presence of tidal turbines caused the displacement of a persistent eddy important to sand bank behaviour and the turbines caused a localised sea bed effects within the development. Furthermore, the results suggested the hydrological changes may influence sediment dynamics of the subtidal features. However, due to the natural variability of the sand wave field, there was discrepancy between observations and the model, highlighting the need for observational data in order to achieve a high level of accuracy. As sediment transport modelling is computationally complex and expensive, along with the costly acquisition of field observations, Gallego et al. (2017) conclude that it would be better to use a generic pragmatic approach and focus detailed efforts on areas where high risk receptors are present. The methodology outlined by Martin-Short et al. (2015) and used here is an example of a generic pragmatic approach. Depth-averaged modelling can provide first stage investigations into the likely performance of a tidal array and its potential impact, identifying areas of greatest risk to changes in bed shear stress. 3D modelling can then be used for detailed site investigations. Within the area of interest for this study, the Pembrokeshire SAC contains grade C sand banks, to the south-west of the Bishop & Clerks, meaning these are of national interest but are not the primary reason for the SAC selection (JNCC, 2015). Results showed that the area of greatest risk to change is within the vicinity of the tidal array with little change to the mean and max bed shear stress over the Pembrokeshire sand banks. The natural variability of the sand banks, due to wave action not considered in this model, is likely to be far higher than the change due to the tidal array.

5 Conclusion

A high-resolution depth averaged hydrodynamic model has been used to simulate the impact of a 10 MW tidal array at Ramsey Sound. The model results show there is a strong disparity between the flood and ebb tide with local bathymetric effects leading to significant differences between the power output of each device. Over the 30-day model run, the tidal array will produce 2.15 GWh, equating to 25.80 GWh per annum. The tidal array impacts the local hydrodynamics by reducing the amplitude of the M2 and S2 tidal constituents by 20% and 19% respectively. Whilst the greatest impact is restricted to the vicinity of the tidal array, far field effects are seen as far as 24km from the site through changes to eddy propagation. Investigations of tidal arrays are particularly site specific and no generic value of impact can be made. If a tidal array is sited such that it does not influence areas of vorticity generation, then impacts can be greatly reduced. However, the sites of interest around the UK are typically in turbulent

environments. The results show the need for higher resolution modelling, at an appropriate scale, to enable the complex features of the environment to be correctly resolved.

However, changes to eddy propagation only provide a short-term view. Eddy propagation is naturally variable due to other atmospheric forcing not included in this model. Benthic species should already be well adapted to highly variable tidal conditions at Ramsey Sound. Therefore, the influence on bed shear stress can provide a better insight into the longer-term impact on morphodynamics. The influence of the array on bed shear stress is more localised and extends to within 12km of the tidal site. Tidal arrays can alter complex hydrodynamic processes and lead to far field effects greater than just the direct wake of the turbines. These alterations could drive changes in bed characteristics and sediment dynamics. Results show the tidal array will lead to localised sediment accumulation and could act as a barrier to sediment transport. Whilst the impact of the 10 MW array is likely to be small, further work is required to determine the ecological response to the change in morphodynamics in Ramsey Sound. Depth-averaged modelling can be a useful tool to provide first stage investigations into the likely performance of a tidal array and its potential impact, identifying areas of greatest risk to changes. These can then be further investigated through the use of more complex 3D modelling.

6 Acknowledgement

The authors thank Cardiff University for providing ADCP data through Ramsey Sound. The work was funded by the Industrial Doctorate Centre for Offshore Renewable Energy which is funded by the Energy Technologies Institute and the RCUK Energy Programme, grant number (EP/J500847/1). This work was carried out on the High Performance Computing Cluster supported by the Research and Specialist Computing Support service at the University of East Anglia.

References

Ahmadian, R. Falconer, R. and Bockelmann-Evans, B., 2012. Far-field modelling of the hydro-environmental impact of tidal stream turbines, Renewable Energy, 38(1), pp.107-116.

Arntz, W.E., Gili, J.M., Reise, K., 1999. Unjustifiably ignored: reflections on the role of benthos in marine ecosystems. In: Gray, J.S. (Ed.). Biogeochemical Cycling and Sediment Ecology. Kluwer Academic, Dordrecht, pp.105-124.

Berenbrock, C. and Tranmer, A.W., 2008. Simulation of flow, sediment transport, and sediment mobility of the lower Coeur d'Alene River, Idaho. US Geological Survey.

Black and Veatch, 2005. Phase 2: UK tidal stream resource assessment. Technical report to Carbon Trust, Report submission 107799/D/2200/03.

British Oceanographic Data Centre, [Online], Available: http://www.bodc.ac.uk/.

Broadhurst, M. and Orme, C.D.L., 2014. Spatial and temporal benthic species assemblage responses with a deployed marine tidal energy device: A small scaled study. Marine environmental research, 99, pp.76-84.

Brown, A.J.G., Neill, S.P. and Lewis, M.J., 2017. Tidal energy extraction in three-dimensional ocean models. Renewable Energy, 114, pp.244-257.

Covich, A.P., Palmer, M.A. and Crowl, T.A., 1999. The role of benthic invertebrate species in freshwater ecosystems: zoobenthic species influence energy flows and nutrient cycling. BioScience, 49(2), pp.119-127.

Cox, A.T. and Swail, V.R., 2001. A global wave hindcast over the period 1958-1997- Validation and climate assessment. Journal of Geophysical Research, 106(C2), pp.2313-2329.

Evans, P., Mason-Jones, A., Wilson, C., Wooldridge, C., O'Doherty, T. and O'Doherty, D., 2015. Constraints on extractable power from energetic tidal straits. Renewable Energy, 81, pp.707-722.

Fairley, I., Neill, S., Wrobelowski, T., Willis, M. and Masters, I., 2011. Potential array sites for tidal stream electricity generation off the pembrokeshire coast. In Proceedings of the 9th European Wave and Tidal Energy Conference, Southampton, UK, pp.5-9.

Fairley, I., Evans, P., Wooldridge, C., Willis, M. and Masters, I., 2013. Evaluation of tidal stream resource in a potential array area via direct measurements. Renewable Energy, 57, pp.70-78.

Gallego, A., Side, J., Baston, S., Waldman, S., Bell, M., James, M., Davies, I., O'Hara Murray, R., Heath, M., Sabatino, A. and McKee, D., 2017. Large scale three-dimensional modelling for wave and tidal energy resource and environmental impact: Methodologies for quantifying acceptable thresholds for sustainable exploitation. Ocean and Coastal Management, 147, pp.67-77.

Haverson, D., Bacon, J., Smith, H.C., Venugopal, V. and Xiao, Q., 2017. Cumulative impact assessment of tidal stream energy extraction in the Irish Sea. Ocean Engineering, 137, pp.417-428.

Heath, M., Sabatino, A., Serpetti, N., McCaig, C. and Murray, R.O.H., 2017. Modelling the sensitivity of suspended sediment profiles to tidal current and wave conditions. Ocean & Coastal Management, 147, pp.49-66.

Hinchey, E.K., Schaffner, L.C., Hoar, C.C., Vogt, B.W. and Batte, L.P., 2006. Responses of estuarine benthic invertebrates to sediment burial: the importance of mobility and adaptation. Hydrobiologia, 556(1), pp.85-98.

Iliffe, J.C., Ziebart, M.K., Turner, J.F., Talbot, A.J. and Lessnoff, A.P., 2013. Accuracy of vertical datum surfaces in coastal and offshore zones. Survey Review, 45(331), pp.254-262.

Joint Nature Conservation Committee., 2015. Pembrokeshire Marine Special Area of Conservation, [Online], Available: http://jncc.defra.gov.uk/protectedsites/sacselection/sac.asp?EUcode=UK0013116.

Keenan, G., Sparling, C., Williams, H. and Fortune, F., 2011. SeaGen environmental monitoring programme final report. Royal Haskoning: Edinburgh, UK, January.

Lewis, M., Neill, S.P., Robins, P.E. and Hashemi, M.R., 2015. Resource assessment for future generations of tidal-stream energy arrays. Energy, 83, pp.403-415.

Martin-Short, R., Hill, J., Kramer, S.C., Avdis, A., Allison, P.A. and Piggott, M.D., 2015. Tidal resource extraction in the Pentland Firth, UK: Potential impacts on flow regime and sediment transport in the Inner Sound of Stroma. Renewable Energy, 76, pp.596-607.

McBreen, F. and Joint Nature Conservation Committee, 2011. UK SeaMap 2010: predictive mapping of seabed habitats in UK waters.

553 Serhadlioglu, S., 2014. Tidal stream resource assessment of the Anglesey Skerries and the Bristol Channel (Doctoral dissertation, University
554 of Oxford).
555 Miller, R.G., Hutchison, Z.L., Macleod, A.K., Burrows, M.T., Cook, E.J., Last, K.S. and Wilson, B., 2013. Marine renewable energy
556 development: assessing the Benthic Footprint at multiple scales. Frontiers in Ecology and the Environment, 11(8), pp.433-440.
557 Neill, S.P., Jordan, J.R. and Couch, S.J., 2012. Impact of tidal energy converter (TEC) arrays on the dynamics of headland sand banks.
558 Renewable Energy, 37(1), pp.387-397.
559 Niclasen, B.A. and Simonsen, K., 2007. Validation of the ECMWF analysis wave data for the area around the Faroe Islands. Societas
560 Scientiarum Færoensis.
561 Pingree, R.D. and Griffiths, D.K., 1979. Sand transport paths around the British Isles resulting from M 2 and M 4 tidal interactions. Journal
562 of the Marine Biological Association of the United Kingdom, 59(02), pp.497-513.
563 Plew, D.R. and Stevens, C.L., 2013. Numerical modelling of the effect of turbines on currents in a tidal channel – Tory Channel, New Zealand,
564 Renewable Energy, 57, p269-282.
565 Rastogi, A.K. and Rodi, W., 1978. Predictions of heat and mass transfer in open channels. Journal of the Hydraulics division, 104(3), pp.397-
566 420.
567 reNEWS. 2014. MCT loses vital Skerries cash, [Online], Avaialble: http://renews.biz/68698/mct-loses-vital-skerries-cash/.
568 RenewableUK, 2015. Wave and Tidal Energy in the UK – Capitalising on Capability, [Online], Available:
569 http://www.renewableuk.com/en/publications/index.cfm/.
570 Robins, P.E., Neill, S.P. and Lewis, M.J., 2014. Impact of tidal-stream arrays in relation to the natural variability of sedimentary processes.
571 Renewable Energy, 72, pp.311-321.
572 Robinson, I.S., 1981. Tidal vorticity and residual circulation. Deep Sea Research Part A. Oceanographic Research Papers, 28(3), pp.195-212.
573 Rogers, C.S., 1990. Responses of coral reefs and reef organisms to sedimentation. Marine ecology progress series. Oldendorf, 62(1), pp.185-
574 202.
575 Shields, M.A., Dillon, L.J., Woolf, D.K. and Ford, A.T., 2009. Strategic priorities for assessing ecological impacts of marine renewable energy
576 devices in the Pentland Firth (Scotland, UK). Marine Policy, 33(4), pp.635-642.
577 Shields, M.A., Woolf, D.K., Grist, E.P., Kerr, S.A., Jackson, A.C., Harris, R.E., Bell, M.C., Beharie, R., Want, A., Osalusi, E. and Gibb, S.W.,
578 2011. Marine renewable energy: The ecological implications of altering the hydrodynamics of the marine environment. Ocean & Coastal
579 Management, 54(1), pp.2-9.
580 Short, F.T. and Wyllie-Echeverria, S., 1996. Natural and human-induced disturbance of seagrasses. Environmental conservation, 23(01),
581 pp.17-27.
582 Soulsby, R., 1997. Dynamics of marine sands: a manual for practical applications. Thomas Telford Publications, London, ISBN 0 7277 2584
583 X, 1997.
584 Thiébot, J., du Bois, P.B. and Guillou, S., 2015. Numerical modeling of the effect of tidal stream turbines on the hydrodynamics and the
585 sediment transport–Application to the Alderney Race (Raz Blanchard), France. Renewable Energy, 75, pp.356-365.
586 Thrush, S.F. and Dayton, P.K., 2002. Disturbance to marine benthic habitats by trawling and dredging: implications for marine biodiversity.
587 Annual Review of Ecology and Systematics, pp.449-473.
588 Tidal Energy Ltd, 2012. Environmental Scoping Report, [Online], Available: http://www.tidalenergyltd.com/.
589 Tidal Energy Ltd, 2015. Wales steps forward in marine renewable energy as the country's first full scale tidal energy demonstration device is
590 installed, [Press Release], 14 December, [Online], Available: http://www.tidalenergyltd.com/?p=2418.
591 Tolman, H.L., 2009. User manual and system documentation of WAVEWATCH III TM version 3.14. Technical note, MMAB Contribution,
592 276, p.220.
593 van Nieuwkoop, J.C., Smith, H.C., Smith, G.H. and Johanning, L., 2013. Wave resource assessment along the Cornish coast (UK) from a 23-
594 year hindcast dataset validated against buoy measurements. Renewable energy, 58, pp.1-14.
595 Walkington, I. and Burrows, R., 2009. Modelling tidal stream power potential. Applied Ocean Research, 31(4), pp.239-245.

- High resolution hydrodynamic model of a 10 MW tidal stream array in near Ramsey Sound
- The tidal array causes a resource reduction of less than 20%
- An array greater than 10MW would risk a greater negative environmental impact
- The tidal array will act as a barrier to sediment transport
- Potential consequences for the benthic ecology of the region